DOI: 10.61782/fa.2023.0435

forum acusticum 2023

EXPERIMENTAL STUDY OF THE IMPEDANCE OF PERFORATED PLATES AT HIGH SOUND PRESSURE AMPLITUDES AND GRAZING FLOW

Ralf Burgmayer[1*] **Karsten Knobloch**[1]

[1] Department of Engine Acoustics, German Aerospace Center, DLR e.V.

ABSTRACT

In this investigation, the impedance of perforated plates subjected to a combination of high amplitude acoustic excitation and a grazing flow is studied experimentally. During the experimental program, the acoustic pressure amplitude is increased stepwise up to approximately 150 dB while the grazing flow speed is varied up to a maximum Mach number of 0.2. Dimensionless variables are used to correlate the change of impedance with the variation of the acoustic excitation amplitude and the grazing flow velocity. Results show that the acoustic excitation only has an effect on the impedance of the perforated plate if the root mean square amplitude of the particle velocity in the holes of the perforate exceeds the threshold of approximately two times the skin friction velocity. For the resistance, an additive relation between the contributions of grazing flow and high-level acoustic excitation can be assumed in case the particle velocity in the orifices exceeds the threshold level. For the reactance, the influence of high-level acoustic excitation above the threshold level is small compared to the influence of the grazing flow.

Keywords: *experimental study, impedance, perforated plate, high sound pressure amplitude, grazing flow.*

**Corresponding author*: *Ralf.Burgmayer@dlr.de.*

1. INTRODUCTION

The jet engine constitutes one of the main sources of noise caused by aviation. One method to reduce the noise emission is to dampen the sound directly in the engine by so called acoustic liners. Most conventional liners function according to a mass spring system and are composed of a perforated facing sheet attached to an assembly of cavities, referred to as honeycomb, terminated by a rigid back plate. The perforated linings are grazed by a continuous flow of high velocity and sound waves of considerable amplitudes. The acoustic characteristics of perforated plates express a dependence on the grazing flow velocity as well as the acoustic particle velocity inside the orifices. Hence, in the design of liners, the knowledge of the interaction of grazing flow and sound waves with high sound pressure is of importance. The acoustic characteristics of such devices are usually described by the acoustic impedance. High sound pressure amplitudes cause flow separation at the edges of the perforations once the particle displacement exceeds the orifice dimensions [1, 2]. The effect was first described by Sivian [3]. The impedance dependent on the sound pressure amplitude is commonly referred to as nonlinear impedance [1]. Due to continuous flow grazing the perforated walls, a turbulent boundary layer forms at the orifices consequently causing a flow through the orifices and flow separation [4]. Modeling the impedance of orifices and perforated plates, the effects of grazing flow and high sound pressure amplitudes are often considered to be independent of each other and therefore contribute to the impedance simultaneously [5–7]. Several studies link the skin friction velocity in the turbulent boundary layer caused by the grazing flow to the changes of impedance and, furthermore, investigate the interaction between high

sound pressure amplitudes and grazing flow. The studies show that the impedance is only dependent on the acoustic particle velocity once its amplitude exceeds a certain threshold value, usually of the magnitude of the skin friction velocity [8–10]. In this manuscript the effect of high amplitude acoustic excitation of perforated plates under grazing flow above this threshold level is studied. Dimensionless quantities are used to first identify the respective threshold value for our experimental facility and, subsequently, to compare the effects of high sound pressure level amplitudes on the impedance with and without grazing flow.

2. EXPERIMENTAL SETUP AND ANALYSIS METHOD

2.1 Experimental setup

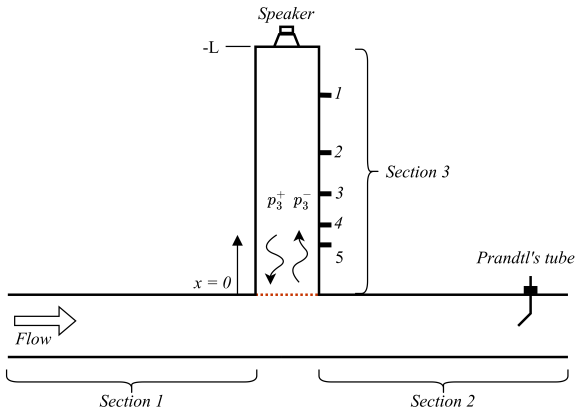

Figure 1. Experimental Setup.

Figure 1 presents the experimental setup. The study is conducted at the rectangular flow duct DUCTR of the department Engine Acoustics of the German Aerospace Center, DLR. Each section of the duct is of width 80 mm and height 60 mm and terminated by an anechoic termination. In the no flow case, the duct features plane wave excitation up to a frequency of approximately 2142 Hz. Grazing flows with maximum flow velocities of $M_{cl} = \frac{u_{cl}}{c_0} \approx 0.3$ can be applied to the main duct via section 1. M_{cl} is the Mach number, u_{cl} refers to the grazing flow velocity measured at the centerline of the duct and c_0 represents the speed of sound. To study the impedance of the perforated plate under grazing flow and high sound pressure amplitudes, a third section is installed between the sections 1 and 2 of the main duct. The perforated plate is mounted flush to the wall at the intersection of the duct segments. Table 1 lists the specifications of the plate. ϕ represents the porosity of the perforated sheet, d the diameter of the orifices and h the thickness of the plate. The acoustic measurements, restricted to plane wave propagation, are conducted in section 3.

The experimental method is based on the assumption that the radiation impedance is independent of the grazing flow in the main duct [11]. According to Ingard and Singhal the assumption is valid for average grazing flow velocities up to $M_{avg} = \frac{u_{avg}}{c_0} \approx 0.2$ [12]. Considering that the effect of both, high sound pressure amplitudes and grazing flow, is to decrease the inertial end correction of the orifices, which constitutes the imaginary part of the radiation impedance [13], the measurement errors are expected to be larger for the reactive part of the impedance, especially for low frequencies and small hole diameters.

2.2 Acoustic measurements

A speaker of type BMS 4599ND is mounted on the rear side of section 3 and five microphones of type GRAS 40BP are mounted flush to the wall. The space between the microphones is reduced logarithmically towards the perforated plate. The sound field, restricted to plane wave propagation, is excited in the form of pure tone stimuli. The study only considers the respective fundamental frequencies of the stimuli, as the effects of uneven higher harmonics, generated at the orifice [14, 15] and the amplitude of distortion introduced by the speaker in the form of even harmonics is, in agreement to previous studies [16], observed to be small compared to the fundamental frequency. The study focuses on measuring the change of impedance due to either grazing flow or high amplitude acoustic actuation or a combination of both effects. Consequently the effects have to be separated. Therefore, in a first step, the linear impedance, i.e. the impedance independent of the sound pressure amplitude, is determined. The linear regime is determined empirically without grazing flow: The sound pressure level is reduced until no change of impedance with sound pressure amplitude is observed. Because the grazing flow in the main duct introduces significant flow noise, the sound pressure was carefully adjusted to maximize the signal to noise ratio. Subsequently, for every grazing flow velocity measured as well as for the no flow case, the sound pressure level at a certain frequency f is increased stepwise from its linear value in order to study the effects of the sound pressure

amplitude on the impedance.

Table 1. Geometric specifications of the perforated plate under study.

Plate	ϕ [%]	d [mm]	h [mm]
P1	4.09	2.5	1

2.3 Analysis of the acoustic measurements

The plane wave sound field in section 3 is transformed into frequency domain by the method of Chung [17] in order to reject flow noise, and is subsequently decomposed into its forward and backwards travelling components. Thereby, thermo-viscous losses at the walls of the duct are incorporated [18]. For an extensive discussion of the analysis method, one should refer to [19]. For each microphone, located at a position x, the sound field can be written as:

$$\hat{p}_3(x) = \hat{p}_3^+ e^{-ik^+x} + \hat{p}_3^- e^{ik^-x}, \tag{1}$$

where the subscript denotes the duct section and the super script the travelling direction of the wave. Using multiple microphones results in an over determined system of equations which is solved for the unknown complex pressure amplitudes of the forward and backward travelling waves $\hat{p}_3^+$ and $\hat{p}_3^-$ at the perforated sheet ($x = 0$). From the plane wave components, the reflection coefficient r is calculated by the common relation $r = \frac{\hat{p}_3^-}{\hat{p}_3^+}$ and, subsequently, the normalized specific impedance ζ is derived by

$$\zeta = \frac{Z}{\rho_0 c_0} = \frac{1-r}{1+r}, \tag{2}$$

where ρ_0 represents the density of air and c_0 is the respective speed of sound. The acoustic particle velocity in the orifices of the facing sheet is given in terms of a root mean square velocity (RMS) and is calculated from the plane wave components at $x = 0$ under the assumption of continuity and by applying Euler's law:

$$|\bar{u}_0| = \frac{|\hat{p}_3^+ - \hat{p}_3^-|}{\rho_0 c_0 \phi \sqrt{2}}. \tag{3}$$

2.4 Grazing flow measurement

The grazing flow velocity at the centerline of the duct u_{cl} is measured by a Prandtl's tube in section 2. From u_{cl} the average flow velocity u_{avg} is derived by nonlinear regression [20]. u_{avg} is estimated in order to comply with the limit of $M_{avg} \leq 0.2$ of the experimental method [11, 12]. Table 2 displays the measured center line Mach numbers M_{cl} and the corresponding approximate average Mach numbers.

Table 2. Average Mach number M_{avg} derived from center line Mach number M_{cl} by nonlinear regression.

M_{cl}	0.05	0.1	0.15	0.2	0.23
M_{avg}	0.045	0.082	0.13	0.17	0.2

In an earlier study flow profiles over the width of the duct have been measured in the hard walled sections of DUCTR [21]. By fitting the measured profiles to the law of the wall, the skin friction velocity u_* at the hard walled section 1 is derived. Fig. 2 displays the calculated skin friction velocity. A linear relationship between u_* and u_{cl} is seen. A linear least squares fit, where the origin is forced to zero, is applied to u_*. The fitting process yields $u_* \approx 0.035 u_{cl}$ m/s. The approximation of u_* is used to relate the measured centerline velocities of this study to the approximate skin friction velocity in the boundary layer of the hard-walled duct.

3. RESULTS

3.1 Resistance

The resistance is depicted as the difference between the resistance at a certain sound pressure and grazing flow velocity $\Re\{\zeta_{fs,GF}\}$ and its linear value at the respective grazing flow velocity $\Re\{\zeta_{lin,GF}\}$ for one orifice:

$$\frac{\Re\{\Delta\zeta\} c_0}{\pi f d} = \frac{\Re\{\zeta_{fs,GF} - \zeta_{lin,GF}\} \phi c_0}{\pi f d} = \frac{\Re\{\Delta Z\}}{\rho_0 \omega r}, \tag{4}$$

where $\omega = 2\pi f$ and r represents the radius of the orifices. Eq. (4) reflects the effects of the high amplitude excitation only. Studies show, that the linear resistance is independent of the interaction between adjacent holes [22,

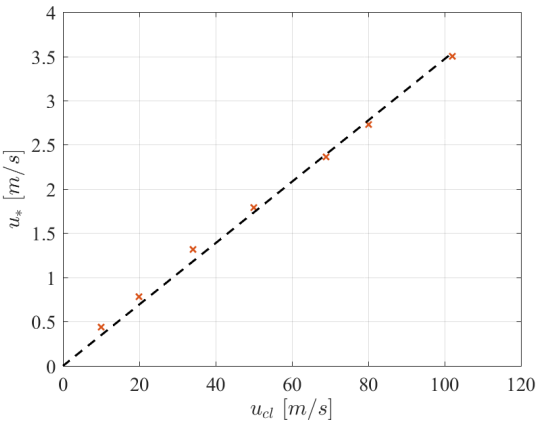

Figure 2. Skin friction velocity u_* at the hard walls of the flow duct. $\times$: Measured $u_{*,meas}$; , $--$: Linear fit $u_{*,fit} \approx 0.035 u_{cl}$ m/s.

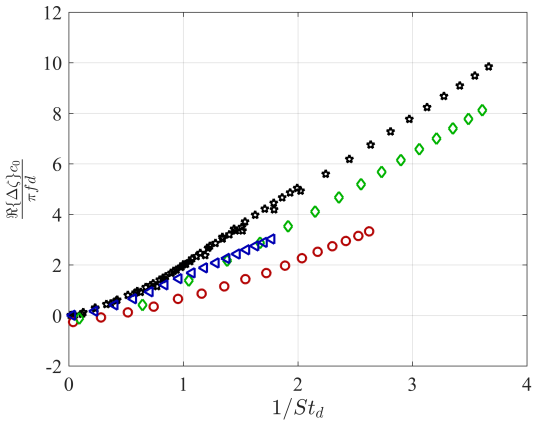

Figure 3. Change of resistance $\frac{\Re\{\Delta\zeta\}\phi c_0}{\pi f d}$ for varying grazing flow velocities and sound pressure amplitudes over $\frac{1}{St_d} = \frac{|\bar{u}_0|}{2\pi f d}$. $\star$: $\frac{\Re\{\Delta\zeta\}c_0}{\pi f d}$ for $M_{avg} = 0$; $\circ$: $\frac{\Re\{\Delta\zeta\}\phi c_0}{\pi f d}$ with $f = 331$ Hz for $M_{avg} \approx 0.2$; $\triangleleft$: $\frac{\Re\{\Delta\zeta\}\phi c_0}{\pi f d}$ with $f = 637$ Hz for $M_{avg} \approx 0.13$; $\diamond$: $\frac{\Re\{\Delta\zeta\}\phi c_0}{\pi f d}$ for $M_{avg} \approx 0.045$.

23], so multiplying $\Re\{\zeta_{fs,GF} - \zeta_{lin,GF}\}$ by ϕ represents the change of resistance of one orifice.

Fig. 3 depicts $\frac{\Re\{\Delta\zeta\}c_0}{\pi f d}$ over the inverse Strouhal number based on the orifice diameter d, $\frac{1}{St_d} = \frac{|\bar{u}_0|}{2\pi f d}$, for a variation of the acoustic particle velocity as well as the grazing flow speed. Compared to the results for $M_{avg} = 0$, we find the particle velocity in the orifices to decrease with increasing Mach number. Due to the grazing flow, the resistance of the perforated sheet increases. The grazing flow is effectively hindering the acoustic flow through the orifice. It is seen that the change of resistance is dependent on the frequency of the impinging sound wave and the grazing flow speed. With decreasing frequency as well as increasing grazing flow, a higher particle velocity $|\bar{u}_0|$ is required to affect the resistance of the perforate. Consequently, the Strouhal number based on the skin friction velocity u_*, $\frac{1}{St_{\tau,d}} = \frac{u_*}{2\pi f d}$, is considered to further evaluate the results.

Fig. 4 depicts $\frac{\Re\{\Delta\zeta\}c_0}{\pi f d}$ over the inverse Strouhal number, built from the difference between $|\bar{u}_0|$ and $2u_*$, $\frac{1}{St_{\Delta\tau,d}} = \frac{|\bar{u}_0| - 2u_*}{2\pi f d}$. The measurements for varying grazing flow velocities and frequencies correlate for the Strouhal number built from the "effective velocity" $(|\bar{u}_0| - 2u_*)$ in the orifice. Three flow regimes can be distinguished: For $|\bar{u}_0| < 2u_*$, the resistance is independent of the acoustic particle velocity. For $|\bar{u}_0| \approx 2u_*$ a transition regime can be identified, where the change of resistance expresses a quadratic dependence on the inverse Strouhal number and comparably small changes in resistance due to the particle velocity in the orifices can be observed. A similar transitional domain is also observed in the case without grazing flow [24]. For $|\bar{u}_0| > 2u_*$, a linear dependence on the inverse Strouhal number and, consequently, on the amplitude of the acoustic particle velocity in the orifice is observed. In this regime, the resistance increases in the same manner as for the case without grazing flow. Thus, an additive relation between the convective parts of the resistance can only be assumed in case the acoustic particle velocity exceeds the skin friction velocity. In the results presented here, the additive relation is valid for $|\bar{u}_0| > 2u_*$. Threshold values of more or less the same order of magnitude are derived in [8–10]. The exact threshold value may vary depending on the duct and measurement method to determine the respective acoustic and skin friction velocity.

3.2 Reactance

The decrease of reactance under flow separation is linked to a loss of end correction. Mass of fluid is dispatched from the orifices by turbulence [9, 24]. We assume the effective inertial length of an orifice L_{in} at high sound pressure amplitudes and grazing flow can be expressed as

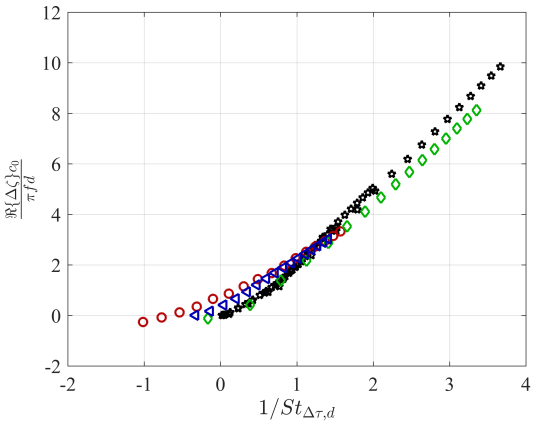

Figure 4. Change of resistance $\frac{\Re\{\Delta\zeta\}\phi c_0}{\pi fd}$ for varying grazing flow velocities and sound pressure amplitudes over $\frac{1}{St_{\Delta\tau,d}} = \frac{|\bar{u}_0|-2u_*}{2\pi fd}$. $\star$: $M_{avg} = 0$; $\circ$: $\frac{\Re\{\Delta\zeta\}\phi c_0}{\pi fd}$ with $f = 331$ Hz for $M_{avg} \approx 0.2$; $\triangleleft$: $\frac{\Re\{\Delta\zeta\}\phi c_0}{\pi fd}$ with $f = 637$ Hz for $M_{avg} \approx 0.13$; $\diamond$: $\frac{\Re\{\Delta\zeta\}\phi c_0}{\pi fd}$ for $M_{avg} = 0.045$.

[25]:

$$L_{in} = h + 2\Delta e\psi l_{fs,GF}. \tag{5}$$

Thereby, $l_{fs,GF} = f(|\bar{u}_0|, u_*)$ represents a loss factor accounting for the decrease of end correction with high sound pressure amplitude and grazing flow. $2\Delta e = \frac{8}{3\pi}d$ describes the external end correction, accounting for mass moving outside of the orifice [26]. In contrast to the resistance, hole interaction has to be considered for the reactance. The hole interaction ψ is incorporated by the function of Fok [27].

l_{fs} can be derived for sole high sound pressure amplitudes, for grazing flow only and for the combined effect respectively by considering the appropriate measurements. The loss of end correction due to sole high sound pressure amplitude excitation, l_{fs}, is derived from the change of reactance with increasing sound pressure amplitude at a certain grazing flow velocity:

$$\frac{\Im\{\zeta_{fs,GF} - \zeta_{lin,GF}\} \cdot \phi}{2He} = \frac{2\Delta e \cdot \psi \cdot (l_{fs} - 1)}{d}, \tag{6}$$

where $He = \frac{\pi fd}{c_0}$ is the Helmholtz number. Solving for l_{fs} gives:

$$l_{fs} = \frac{\Im\{\zeta_{fs,GF} - \zeta_{lin,GF}\} \cdot \phi \cdot d}{2He \cdot 2\Delta e \cdot \psi} + 1. \tag{7}$$

Redefining Eq. (7) by always using the linear no flow reactance as reference gives the combined influence of the high amplitude effects and the grazing flow on the end correction $l_{fs,GF}$:

$$l_{fs,GF} = \frac{\Im\{\zeta_{fs,GF} - \zeta_{lin,GF=0}\} \cdot \phi \cdot d}{2He \cdot 2\Delta e \cdot \psi} + 1. \tag{8}$$

Analogous to Eqs. (7) and (8), by building the difference only using measurements at low sound pressure amplitudes and varying the grazing flow velocity, the loss of end correction due to grazing flow exclusively l_{GF} can be derived.

$$l_{GF} = \frac{\Im\{\zeta_{lin,GF} - \zeta_{lin,GF=0}\} \cdot \phi \cdot d}{2He \cdot 2\Delta e \cdot \psi} + 1. \tag{9}$$

In contrast to the resistance, the Strouhal number on the basis of the plate thickness h, $\frac{1}{St_{\Delta\tau,h}} = \frac{|\bar{u}_0|-2u_*}{2\pi fh}$, is used to display the results. h appears to be the relevant length scale when comparing the end correction of orifices and perforated plates with varying geometric properties under grazing flow and high sound pressure amplitudes [9].

Fig. 5 depicts the loss of end correction l_{fs} due to high amplitude excitation only, as defined in Eq. (7), for various grazing flow velocities. Without grazing flow, l_{fs} decreases and rapidly approaches a plateau value of approximately 0.5. Hence, the end correction is reduced to approximately one half of its linear value due to high sound pressure amplitudes, as qualitatively assumed by Ingard and Ising [14]. Under grazing flow, the loss of end correction due to the high sound pressure amplitude is decreased, dependent on $\frac{1}{St_{\tau,h}} = \frac{u_*}{2\pi fd}$. For $\frac{1}{St_{\tau,h}} > 0.3$, the end correction is independent of the sound pressure amplitude as $l_{fs} \approx 1$. Thus, the end correction does not decrease with increasing sound pressure amplitude once a certain $\frac{1}{St_{\tau,h}}$ and, respectively, a certain grazing flow velocity is attained. The different flow regimes observed for the resistance can also be related to the behavior of the end correction: In case $|\bar{u}_0| < 2u_*$, no end correction is lost due to the acoustic excitation, since the effects of grazing flow are dominant. For $\frac{1}{St_{\Delta\tau,h}} \approx 0$, the dependence on $|\bar{u}_0|$ starts to develop and the end correction (for small $\frac{1}{St_{\tau,h}} < 0.3$) decreases with $|\bar{u}_0|$. A slight increase

in end correction is observed to mark the beginning of the transition regime. An increased end correction is also reported for high amplitude acoustic excitation without grazing flow and is connected to vortex formation at the orifices without separation of the flow [24]. Consequently, the increase in end correction observed here might be for the same reason. For $\frac{1}{St_{\Delta\tau,h}} > 0$ (and small $\frac{1}{St_{\tau,h}} < 0.3$), the end correction approximates a plateau value. Thereby, the smaller $\frac{1}{St_{\tau,h}}$, the higher is the correlation of l_{fs} to the case without grazing flow. The question why no loss of end correction due to acoustic excitation is observed for $\frac{1}{St_{\tau,h}} > 0.3$ remains.

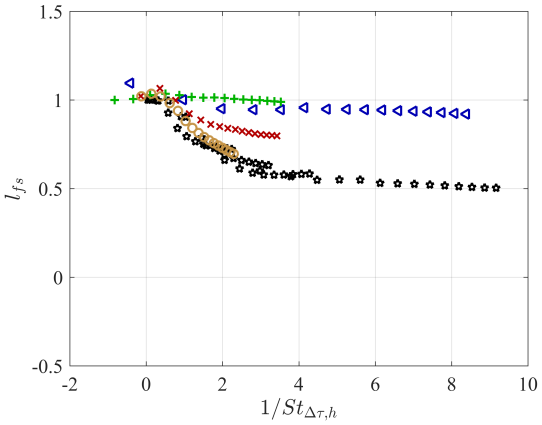

Figure 5. Change of end correction due to high sound pressure amplitudes l_{fs} for varying grazing flow velocities over $\frac{1}{St_{\Delta\tau,h}} = \frac{|\bar{u}_0|-2u_*}{2\pi fh}$. $\star$: $\frac{1}{St_{\tau,h}} = 0$; $\circ$: $\frac{1}{St_{\tau,h}} \approx 0.085$ $\times$: $\frac{1}{St_{\tau,h}} \approx 0.11$; $\triangleleft$: $\frac{1}{St_{\tau,h}} \approx 0.32$; $+$: $\frac{1}{St_{\tau,h}} \approx 0.45$.

Fig. 6 depicts $l_{fs,GF}$ and l_{GF} over $\frac{1}{St_{\tau,h}} = \frac{u_*}{2\pi fh}$. The $\star$-Symbols represent l_{GF}. The solid lined curve, following the grazing flow only results, represents its respective empirical approximation:

$$l_{GF} = \frac{0.14}{0.14 + 1/St_{\tau,h}^2}. \tag{10}$$

Eq. (10) was derived by fitting the function $l_{GF} = \frac{\kappa}{\kappa+1/St_{p,h}^2}$ with the free variable κ to the measurement results by applying the Nelder-Mead-Simplex method [28]. The remaining symbols depict results for measurements at their maximum acoustic particle velocity in the orifices and the same respective grazing flow velocities as presented in Fig. 5. Moreover, additional results for two measurements, conducted at their respective maximum acoustic particle velocities and higher grazing flow velocities, are presented ($\square$ and $\diamond$ symbols).

The end correction for the case of grazing flow only decreases quickly with increasing u_*. For $\frac{1}{St_{\tau,h}} \approx 1$, the end correction is almost completely lost as l_{GF} approximates zero. Comparing the loss of end correction for only grazing flow to the combined effect conveys the small influence the acoustic excitation has on the end correction, especially when grazing flow is present. The end correction is almost completely lost due to the grazing flow. For $\frac{1}{St_{\tau,h}} \approx 0.32$ ($\triangleleft$ symbol), $l_{GF} \approx 0.5$ roughly corresponds to the plateau value of the loss of end correction at mere acoustic excitation and zero grazing flow, see $\star$ symbols in Fig. 5. Thus, it is assumed that only a certain amount of external mass can be convected away from the orifices by acoustically excited flow separation, and, once this value is attained, the acoustic excitation induces no further loss in end correction. This would explain why no loss of end correction can be observed for measurements with $\frac{1}{St_{\tau,h}} > 0.3$ despite considerable acoustic particle displacement being prevalent in the orifices ($\frac{1}{St_h} > 1$).

4. CONCLUSIONS

This study concerns the effect of high amplitude acoustic actuation on the impedance of perforated plates under grazing flow. The results demonstrate that the impedance of perforated plates is independent of the acoustic excitation amplitude in case the amplitude of the acoustic particle velocity in the orfices of the plate $|\bar{u}_0|$ is smaller than two times the skin friction velocity u_*, measured in the hard walled part of the flow duct. Based on the threshold of $2u_*$, three flow regimes are distinguished. For $|\bar{u}_0| < 2u_*$, the grazing flow dominates and the impedance is only dependent on the velocity of the grazing flow. For $|\bar{u}_0| \approx 2u_*$ a transition takes place, where a dependence of the impedance on the acoustic particle velocity in the orifices develops. For $|\bar{u}_0| > 2u_*$, the impedance expresses a dependence on the sound pressure amplitude. While the influence of the sound pressure amplitude on the resistance can be quite large under grazing flow, the reactance only shows a small dependence on the sound pressure amplitude, because a considerable part of the end correction is already lost due to the grazing flow.

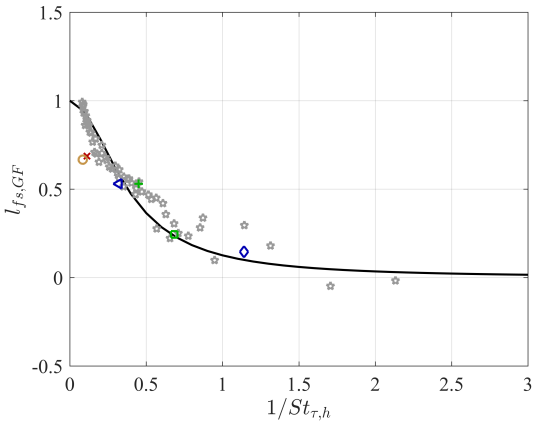

Figure 6. Change of end correction due to sole grazing flow l_{GF} compared to the change of end correction for a combination of grazing flow and high sound pressure amplitudes $l_{fs,GF}$ over $\frac{1}{St_{\tau,h}} = \frac{u_*}{2\pi fh}$. $\star$: $\frac{1}{St_h} \ll 0.5$ $\circ$: $\frac{1}{St_h} \approx 2.46$ $\times$: $\frac{1}{St_h} \approx 3.65$; $\triangleleft$: $\frac{1}{St_h} \approx 9.03$; $+$: $\frac{1}{St_h} \approx 4.43$; $\square$: $\frac{1}{St_h} \approx 3.78$; $\diamond$: $\frac{1}{St_h} \approx 7.27$.

5. REFERENCES

[1] U. Ingard and S. Labate, "Acoustic circulation effects and the nonlinear impedance of orifices," *Journal of the Acoustical Society of America*, vol. 22, pp. 211–218, 1950.

[2] G. B. Thurston and C. E. Martin, "Periodic fluid flow through circular orifices," *The Journal of the Acoustical Society of America*, vol. 25, no. 1, pp. 26–31, 1953.

[3] L. J. Sivian, "Acoustic impedance of small orifices," *The Journal of the Acoustical Society of America*, vol. 7, no. 2, pp. 94–101, 1935.

[4] U. Ingard, "Absorption characteristics of nonlinear acoustic resonators," *The Journal of the Acoustical Society of America*, vol. 44, no. 4, pp. 1155–1156, 1968.

[5] E. Feder and L. W. Dean, "Analytical and experimental studies for predicting noise attenuation in acoustically treated ducts for turbofan engines," *NASA CR-1373*, September 1969.

[6] A. Guess, "Calculation of perforated plate liner parameters from specified acoustic resistance and reactance," *Journal of Sound and Vibration*, vol. 40, no. 1, pp. 119–137, 1975.

[7] A. Cummings and W. Eversman, "High amplitude acoustic transmission through duct terminations: Theory," *Journal of Sound and Vibration*, vol. 91, no. 4, pp. 503–518, 1983.

[8] A. L. Goldman and R. L. Panton, "Measurement of the acoustic impedance of an orifice under a turbulent boundary layer," *The Journal of the Acoustical Society of America*, vol. 60, no. 6, pp. 1397–1405, 1976.

[9] J. Kooi and S. Sarin, *An experimental study of the acoustic impedance of Helmholtz resonator arrays under a turbulent boundary layer*. AIAA 1981-1998, 1981.

[10] C. Malmary, S. Carbonne, Y. Auregan, and V. Pagneux, *Acoustic impedance measurement with grazing flow*. AIAA 2001-2193, 2001.

[11] G. Kooijman, A. Hirschberg, and J. Golliard, "Acoustical response of orifices under grazing flow: Effect of boundary layer profile and edge geometry," *Journal of Sound and Vibration*, vol. 315, no. 4, pp. 849–874, 2008.

[12] U. Ingard and V. K. Singhal, "Upstream and downstream sound radiation into a moving fluid," *The Journal of the Acoustical Society of America*, vol. 54, no. 5, pp. 1343–1346, 1973.

[13] P. M. Morse and K. U. Ingard, *Theoretical Acoustics*. Princeton University Press, 1968.

[14] K. U. Ingard and H. Ising, "Acoustic nonlinearity of an orifice," *The Journal of the Acoustical Society of America*, pp. 6–17, 1967.

[15] N. S. Dickey and A. Selamet, "Acoustic nonlinearity of a circular orifice: An experimental study of the instantaneous pressure/flow relationship," *Noise Control Engineering Journal*, vol. 46, no. 3, pp. 97–107, 1998.

[16] U. Ingard, "Nonlinear distortion of sound transmitted through an orifice," *The Journal of the Acoustical Society of America*, vol. 48, no. 1A, pp. 32–33, 1970.

[17] J. Y. Chung, "Rejection of flow noise using a coherence function method," *The Journal of the Acoustical Society of America*, vol. 62, no. 2, pp. 388–395, 1977.

[18] E. Dokumaci, "A note on transmission of sound in a wide pipe with mean flow and viscothermal attenuation," *Journal of Sound and Vibration*, vol. 208, pp. 653–655, 1997.

[19] C. Lahiri, *Acoustic performance of bias flow liners in gas turbine combustors*. PhD thesis, Technical University Berlin, Berlin, Germany, 2013.

[20] D. Ronneberger, *Theoretische und experimentelle Untersuchung der Schallausbreitung durch Querschnittssprünge und Lochplatten in Strömungskanälen ; Abschlussbericht zum DFG-Forschungsvorhaben "Akustische Reflexion ..."*. DFG, 1987.

[21] A. Schulz, C. Weng, F. Bake, L. Enghardt, and D. Ronneberger, *Modeling of liner impedance with grazing shear flow using a new momentum transfer boundary condition*. AIAA 2017-3377, 2017.

[22] M. A. Temiz, I. L. Arteaga, G. Efraimsson, M. Åbom, and A. Hirschberg, "Acoustic end correction in micro-perforated plates : revisited," in *The 21st International Congress on Sound and Vibration*, 2014.

[23] V. Naderyan, R. Raspet, C. Hickey, and M. Mohammadi, "Acoustic end corrections for micro-perforated plates," *The Journal of the Acoustical Society of America*, vol. 146, pp. EL399–EL404, 10 2019.

[24] M. A. Temiz, J. Tournadre, I. L. Arteaga, and A. Hirschberg, "Non-linear acoustic transfer impedance of micro-perforated plates with circular orifices," *Journal of Sound and Vibration*, pp. 418–428, 2016.

[25] R. Burgmayer, F. Bake, and L. Enghardt, "Reduction of inertial end correction of perforated plates due to secondary high amplitude stimuli," *JASA Express Letters*, vol. 2, no. 4, p. 042801, 2022.

[26] J. W. Strutt and B. Rayleigh, *The Theory of Sound Volume II*. Macmillan, 1929.

[27] V. A. Fok, "Theoretical study of the conductance of a circular hole, in a partition across a tube," in *Proceedings of the USSR Academy of Sciences*, vol. 31, pp. 875–878, 1941.

[28] J. C. Lagarias, J. A. Reeds, M. H. Wright, and P. E. Wright, "Convergence properties of the nelder-mead simplex method in low dimensions," *SIAM Journal of Optimization*, vol. 9, pp. 112–147, 1998.